RESTORING FORCE CHARACTERISTICS AND MODEL OF HIGH-STRENGTH CONCRETE FILLED STEEL TUBE COLUMN

Motoo SAISHO[1] And Teruo MATSUYAMA[2]

SUMMARY

A restoring force model of concrete filled steel tube column (CFT column) is obtained from the cyclic loading test of CFT column. The restoring force model is composed of the Tri-linear model and the modified Clough model and easily applicable to seismic response numerical analysis of CFT frame under strong ground motion. The proposed model is defined by the yield strength, the ultimate strength and the accumulated plastic deformation capacity of CFT column. The equations to express these characteristics of CFT column are also derived from the test results. By calculating the energy absorbing capacity and comparing it with the test results it is ascertained that the presented model can predict well the restoring force characteristics of CFT column.

INTRODUCTION

The restoring force characteristics of concrete filled steel tube column (CFT column) under dynamic cyclic load indicate considerable ductility without strength loss and CFT column is expected to work as effective seismic-resistant member. But the restoring force characteristics of it are complicated because of the confine effect of concrete, the two dimensional stress of steel tube, the loading rate effect, the local buckling and the crack of steel tube [Saisho and Mitsunari, 1992], [Mitsunari and Saisho, 1996], [Saisho et al,1999a]. To analyze the seismic response of CFT frame under strong ground motion strictly the restoring force model which can calculate the effects of the behaviors mentioned above is required.
From this reason the restoring force model of CFT column which is composed of the Tri-linear model and the modified Clough model [Umemura et al, 1982] and easily applied to seismic response analysis is derived from dynamic loading test of CFT column. The presented model is determined by the characteristics of CFT column which are the elastic stiffness, the yield strength, the ultimate strength and the accumulated plastic deformation capacity. The equations to express these characteristics are also derived on the basis of test result. The usefulness of the presented restoring force model is examined by calculating the energy absorbing capacity of CFT column and comparing it with the test results.

2. DYNAMIC AND STATIC LOADING TEST

2.1 CFT column specimen and test conditions

Dynamic and static loading tests of CFT column have been carried out. The specimens are the cross-formed type explained in Figure 1 which are composed of CFT column and H section steel beam. The effects of the material and the diameter to thickness ratio of steel tube, the filled concrete strength, the axial force ratio, the column length, the loading rate and the hysteresis of column deformation on the restoring force characteristics have been investigated. The steel tube of CFT column is the cold-formed circular steel tube, the sections of which are

[1] *Dept. of Architecture and Civil Engineering, Kumamoto University, Japan Email: saisho@gpo.kumamoto-u.ac.jp*
[2] *Dept. of Architecture and Civil Engineering, Kumamoto University, Japan*

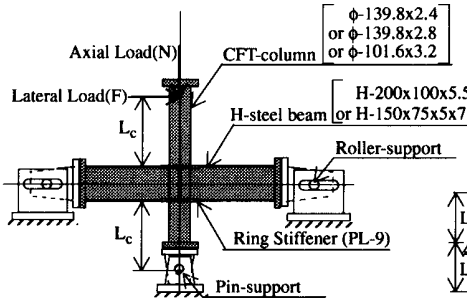

Figure 1: CFT specimen

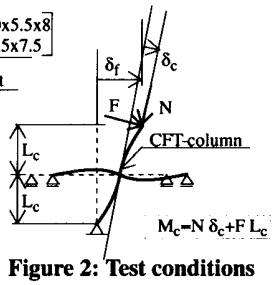

Figure 2: Test conditions

Table 1: Material properties of steel tube

Circular steel tube	σ_y	σ_u	ε_f
φ-101.6x3.2	3.85	4.64	30.7
φ-139.8x2.8	3.48	4.52	34.3
φ-139.8x2.4	4.72	5.60	26.7

σ_y : yield stress (tf/cm^2)
σ_u : tensile strength (tf/cm^2)
ε_f : fracture strain (%)

φ-139.8x2.4, φ-139.8x2.8 and φ-101.6x3.2. The material properties are shown in Table 1.
The loading condition and the support condition of test are mentioned in Figure 1-Figure 2. The column-end is pin-supported and the constant axial load (N) is applied to the another column-end. The beam-ends are roller-supported. To test the response behavior of CFT column under strong seismic load, the cyclic lateral load (F) is also given by the use of an actuator. There are three kinds of time-histories of the lateral displacement at the loading point (δ_f). They are the random wave and the sinusoidal waves with constant amplitude and gradually increasing amplitude. Under dynamic load the maximum velocity of the lateral displacement ($d\delta_f/dt$) and the maximum strain rate of steel tube were 10cm/second and 0.1/second-0.3/second respectively. In dynamic loading test the measured data were acquired in every 0.01second. In static loading test the small incremental lateral displacement ($\Delta\delta_f$) was applied to CFT column and the deformation was kept stationary for one minute to exclude the loading rate effect on the restoring force. After the loading rate effect was fully excluded the measured data were acquired and the next incremental small displacement was applied to the specimen. Static loading test was carried out by repeating this loading process.

2.2 Load-deformation relation of CFT specimen

Load-deformation relations are shown in Figure 3-Figure 4. The load (M_c) is the bending moment at the column-end and the deformation (δ_c) is the deflection of column as shown in Figure 2. In Figure 3-Figure 4 the arrows indicate the points of the maximum load (M_m), the local buckling (LB) and the crack of steel tube (Crack) respectively. The local buckling of steel tube has been observed by the use of wire strain gages attached to the surface of steel tube 25mm apart from the column-end as explained in Figure 5. Before the steel tube buckles locally the surface axial strain of steel tube (ε_A) is nearly proportional to the column deformation (δ_c). When the steel tube buckles locally the incremental surface strain changes from the minus value to the plus value as shown in Figure 5.
While the deformation of CFT column is small, the load-deformation relation of CFT column is spindle-shaped. After the local buckling of steel tube the stiffness of load-deformation relation deteriorates obviously but the

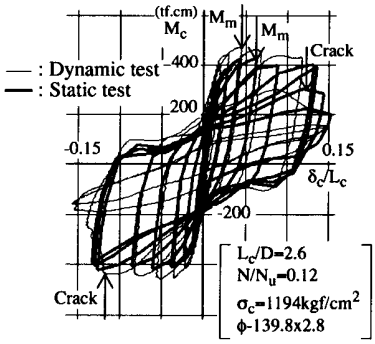

Figure 3: Load-deformation relations of dynamic test and static test

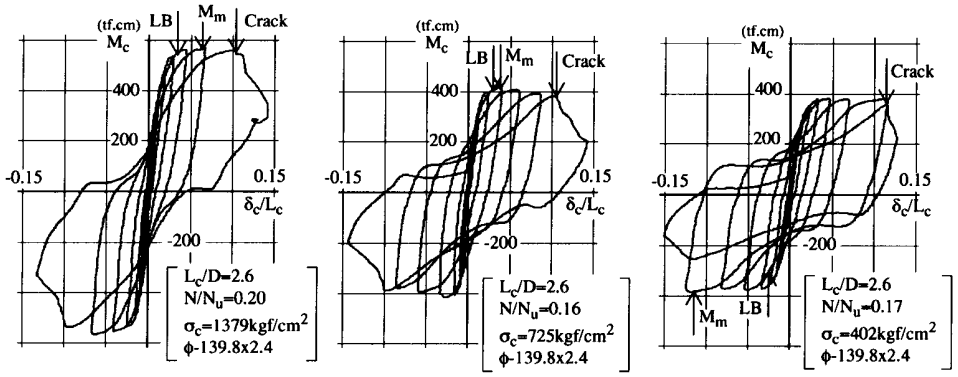

Figure 4: Load-deformation relations of variable concrete filled specimens (LB: Local buckling, Crack: Crack of steel tube, M_m: The maximum load)

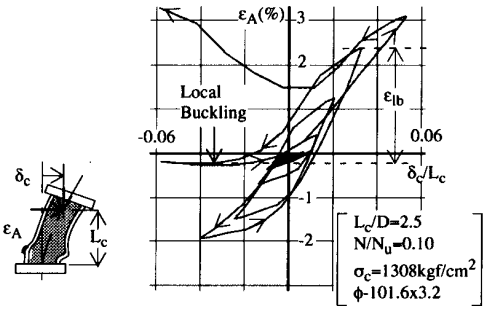

Figure 5: Relation between axial strain and local buckling of steel tube

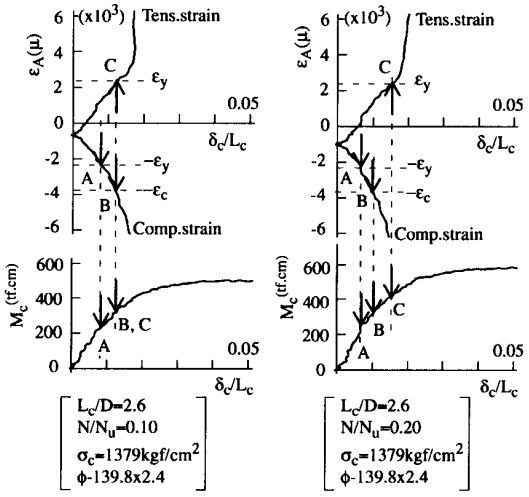

Figure 6: Relation between axial strain of steel tube and bending moment of CFT column

maximum load in every cycle does not decrease. Finally the steel tube cracked in the cross section near the column-end and the restoring force lowered extremely. Accordingly the crack of steel tube indicates the ultimate state of CFT column. In the CFT column test the cyclic loading of every specimen continued until it fails completely and all specimens in this paper have cracked at the ultimate state.

3. RESTORING FORCE CHARATERISTICS OF CFT COLUMN

3.1 Yield strength of CFT column

Figure 6 shows the relations between the axial strain of steel tube (ε_A) and the bending moment at the column-end. The points A and C indicate the yielding of steel tube in compression and in tension respectively. The point B indicates the concrete strain has reached to the ultimate strain (ε_c). When the axial tension strain of steel tube reaches to the yield strain (ε_y) the axial strain increases remarkably and the stiffness of CFT column gradually deteriorates. From this behavior the point C corresponds to the yield strength of CFT column ($_cM_y$). The bending moment ($_cM_y$) when the steel tube yields in tension is obtained from the test results and compared with the calculated yield strength of CFT column (M_y) as shown in Figure 7. In the figure M_y is calculated by the generalized superposed strength method assuming the stress distributions of steel tube and filled concrete are triangular and the maximum stresses of them are equal to the yield stress (σ_y) and the concrete strength (σ_c) respectively. The average values of $M_y/{}_cM_y$ distribute linearly as shown by the dashed line in Figure 7 and the yield strength of CFT column M_{ye}($=_cM_y$) is approximated by Eq.(1).

$$M_{ye}=M_y/(0.19\rho+0.80) \quad (1)$$

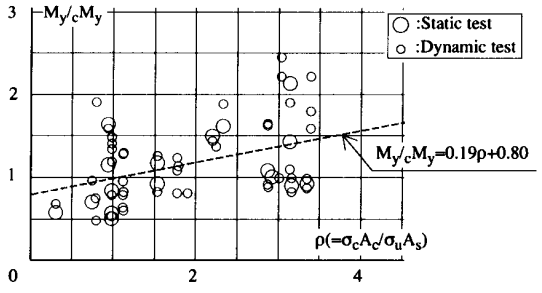

Figure 7: Yield strength by the test results and the generalized superposed strength method

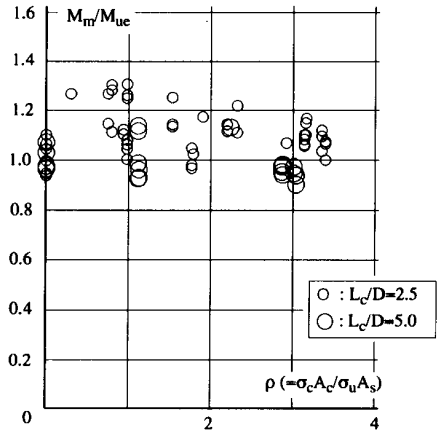

Figure 8: Ultimate strength by the test results and the generalized superposed strength method

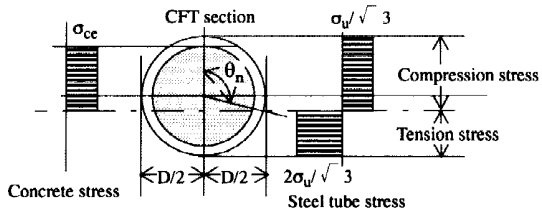

Figure 9: Stress distribution at the ultimate state

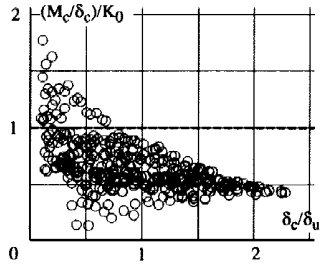

Figure 10: Elastic stiffness of CFT column

in which $\rho=\sigma_c A_c/\sigma_u A_s$ (σ_c:the concrete strength, σ_u:the tensile strength of steel tube, A_c, A_s:the sectional areas of concrete and steel tube). The loading rate effect on the yield strength is indicated in Figure 7. But it is neglected in Eq.(1) because the loading rate effect is not observed clearly in Figure 7.

3.2 Ultimate strength of CFT column

The maximum bending moments of CFT specimen (M_m) are compared with the calculated ultimate strength (M_{ue}) in Figure 8. The abscissa ρ is the strength ratio of the filled concrete to the steel tube of CFT column. M_{ue} is obtained by the generalized superposed strength method expressed by Eq.(2) assuming that the stress distribution are rectangular at the ultimate state as shown in Figure 9.

$$M_{ue}={}_cM_{ue}+{}_sM_{ue}, \qquad N={}_cN_e+{}_sN_e \tag{2}$$

in which ${}_cM_{ue}$, ${}_sM_{ue}$ the ultimate bending strength of filled concrete and steel tube and ${}_cN_e$, ${}_sN_e$ are the axial force of filled concrete and steel tube. In the assumed stress distribution the confined concrete stress is σ_{ce} ($=\sigma_c$ (0.76/ ρ+0.76)) and the steel tube stress in tension and compression are $2\sigma_u/\sqrt{3}$ and $\sigma_u/\sqrt{3}$ respectively [Saisho et al, 1999b]. The loading rate effect on M_{ue} is also considered by increasing it by 10% on the basis of test results [Saisho and Mitsunari, 1999a]. From the results in Figure 8 it is ascertained that the maximum strengths of CFT specimen are well predicted by M_{ue}.

3.3 Elastic stiffness of CFT column

The elastic stiffness of CFT column (K_0) in the relation between δ_c and M_c is expressed by Eq.(3)

$$K_0 = \frac{1}{\frac{L_c^2}{3E_sI_s}+\frac{\gamma_s}{G_sA_s}} + \frac{1}{\frac{L_c^2}{3E_cI_c}+\frac{\gamma_c}{G_cA_c}} \tag{3}$$

in which E_sI_s, E_cI_c:the bending stiffness, G_s, G_c:the shear moduli of steel tube and filled concrete respectively and $\gamma_s=4/3(D^2+Dd+d^2)/(D^2+d^2)$, $\gamma_c=4/3$ (γ_s, γ_c: the moduli of section, D, d: the outside and inside diameter of steel tube). In Eq.(3) it is assumed that there is not the friction between filled concrete and steel tube and the warping in the column-end section caused by shear strain is not constrained. The stiffness of CFT specimen (M_c / δ_c) is compared with the calculation of K_0 in Figure 10 in which $\delta_u=M_{ue}/K_0$. As the deformation of CFT column increases the stiffness of it deteriorates extremely and it can not be expressed by constant value. The stiffness K_0 is corresponding to the average value of M_c / δ_c when the deformation of CFT column is small enough.

3.4 Local buckling of steel tube

The steel tube of CFT column is prevented by filled concrete to deform freely. Due to this behavior the steel tube of specimen did not buckle locally before the column fully yielded and the plastic strain was accumulated in the steel tube. Figure 11 shows the plastic axial strain (ε_{lb}) when the local buckling of steel tube observed in the test. The plastic strain ε_{lb} is the plastic axial strain amplitude when local buckling generated as explained in Figure 5. According to Figure 11 the values of $\varepsilon_{lb}/(\sigma_u/E_s)$ (E_s:the Young's modulus of steel tube) are nearly constant and the average values of them are approximated by Eq.(4)

$$\varepsilon_{lb}=14\,\sigma_u/E_s \tag{4}$$

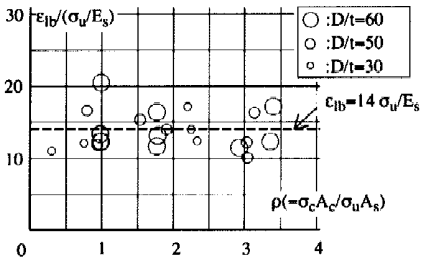

Figure 11: Compression strain amplitude at local buckling of steel tube

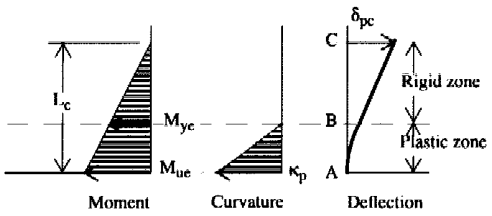

Figure 12: Assumed plastic deformation of column

To express ε_{lb} with the deformation of column the relation between the axial plastic strain and the plastic deformation of CFT column is derived. If the moment and the curvature of plastic deformation (κ_p) distribute linearly as shown in Figure 12, the plastic deformation ratio μ ($=\delta_{pc}/\delta_u$) of CFT column can be expressed by Eq.(5).

$$\frac{D}{2}\kappa_p = \beta\mu \quad \text{in which} \quad \beta = \frac{3}{(1-M_{ye}/M_{ue})(2+M_{ye}/M_{ue})}\frac{D\delta_u}{L_c^2} \tag{5}$$

If the position of neutral axis in the CFT column section is expressed by θ_n as shown in Figure 9, it is decided by Eq.(6) which shows the equilibrium condition of axial force.

$$\pi(1+\rho)\frac{N}{N_u} - \frac{1}{\sqrt{3}}(3\theta_n - 2\pi) - r\rho(\theta_n - \sin\theta_n\cos\theta_n) = 0 \tag{6}$$

in which N: axial force, $N_u=\sigma_c A_c+\sigma_u A_s$, $\gamma=\sigma_{ce}/\sigma_c$ (=0.76/ ρ+0.76) [Saisho et al, 1999b]. If the column cross section assumed to be plane, the axial strain of steel tube (ε_A) can be determined by the curvature (κ_p) expressed by μ and the position of neutral axis (θ_n) at the CFT column-end which are given by Eq.(5) and Eq.(6). The derived ε_A-μ relation is applied to Eq.(4) and we get Eq.(7).

$$\mu_{LB} = \frac{1}{1-\cos\theta_n}\frac{s\cdot\varepsilon_{lb}}{\beta} + \frac{1+\cos\theta_n}{1-\cos\theta_n}\mu_T \tag{7}$$

in which s=1 when $M_c>1$ and s=-1 when $M_c<0$. The value of μ_T is the plastic deformation ratio at the maximum tension strain before the local buckling. Eq.(7) gives the plastic deformation ratio μ_{LB} when the steel tube buckles locally. The accumulated deformation ratio $\Sigma|\Delta\delta_c|/\delta_u$ ($\Delta\delta_c$: incremental deformation, Σ: summation of increment) of every CFT specimen until the steel tube buckles is compared with the prediction by Eq.(7) in Figure 13. The predictions by Eq.(7) are nearly corresponding to the lower limit of the test results.

3.5 Accumulated plastic deformation capacity of CFT column

The accumulated plastic deformation capacity of CFT column (μ_{cr}) is derived here. The value of μ_{cr} is the summation of incremental plastic deformation ratio ($\Sigma|\Delta\delta_p|/\delta_u$) until the steel tube cracks in the cross section near the column-end. The incremental plastic deformation ($\Delta\delta_p$) is mentioned in Figure 15. To determine the capacity it is assumed that the steel tube cracks when the accumulated surface plastic tension strain becomes equal to the characteristic critical value of steel tube as shown Eq.(8).

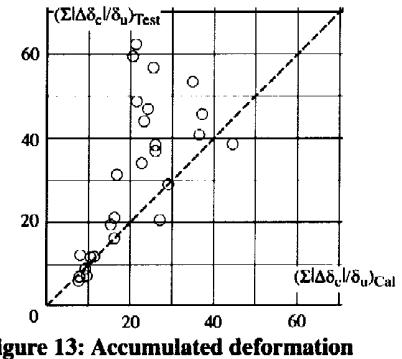

Figure 13: Accumulated deformation until steel tube buckles locally

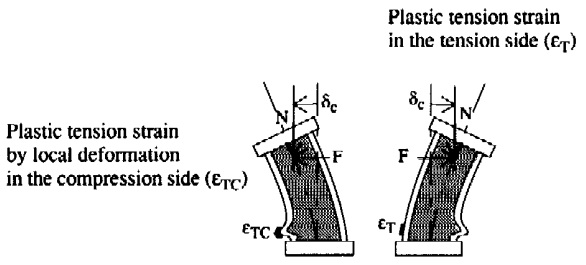

Figure 14: Plastic tension strain on the surface of steel tube

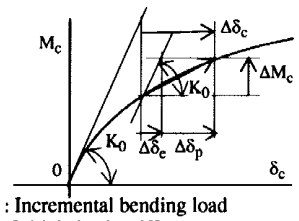

ΔM_c : Incremental bending load
K_0 : Initial elastic stiffness
$\Delta\delta_c$: Incremental deformation
$\Delta\delta_e(=\Delta M_c/K_0)$: Incremental elastic deformation
$\Delta\delta_p(=\Delta\delta_c-\Delta\delta_e)$: Incremental plastic deformation

Figure 15: Incremental deformation ($\Delta\delta_c$) and incremental plastic deformation ($\Delta\delta_p$)

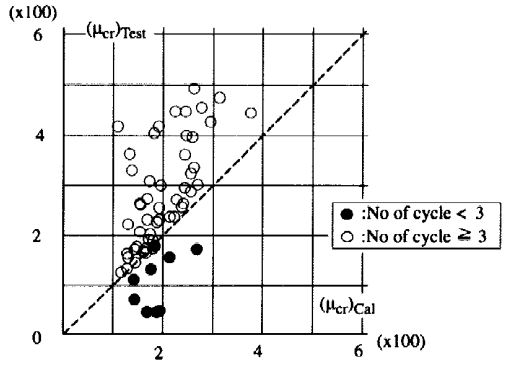

Figure 16: Accumulated plastic deformation capacity

$$\Sigma \varepsilon_T + \Sigma \varepsilon_{TC} = \alpha \varepsilon_f \tag{8}$$

in which ε_T is the surface plastic tension strain of steel tube when it is in the tension side of CFT column. ε_{TC} is also the surface plastic tension strain of steel tube when it is in the compression side of CFT column and the local buckling is generated as explained in Figure 14. Σ means the summation of the plastic tension strain in every load cycle until the steel tube cracks. ε_f is the fracture strain of steel tube. α is the constant to express the effect of the characteristic stress distribution of CFT column and the cyclic loading on the steel tube crack. The equation of α has been obtained as $\alpha = -0.3\rho+5.0$ [Saisho et al, 1999c]. After the plastic tension strains ε_T and ε_{TC} are expressed by the plastic deformation ratio μ ($=\delta_{pc}/\delta_u$) of CFT column by the use of Eq.(5) and Eq.(6), Eq.(9) is derived from Eq.(8) to give the accumulated plastic deformation capacity of CFT column (μ_{cr}).

$$\sum_j (1+\cos\theta_n)\beta\mu_{Tj} + \sum_j \frac{\pi t}{l_{lb}}\sqrt{(1-\cos\theta_n)\beta}\sqrt{\mu_{TCj}} = \alpha\varepsilon_f \tag{9}$$

in which μ_{Tj} is the plastic deformation ratio to generate the surface plastic tension strain of steel tube ε_T and μ_{TCj} is also the plastic deformation ratio to generate the surface plastic tension strain of steel tube ε_{TC} in the j-cycle of lateral loading. In Eq.(9) t and l_{lb} are the thickness and the elastic local buckling length of steel tube respectively. The accumulated plastic deformation capacity of CFT column (μ_{cr}) is expressed by the summation ($\Sigma\mu_{Tj}+\Sigma\mu_{TCj}$). The calculated values $(\mu_{cr})_{Cal}$ are compared with the accumulated plastic deformation capacity of CFT specimen $(\mu_{cr})_{Test}$ in Figure 16. It is shown that the calculated values $(\mu_{cr})_{Cal}$ are corresponding to the lower limit of the test results $(\mu_{cr})_{Test}$ except the extraordinary low cycle failure cases.

4. RESTORING FORCE MODEL OF CFT COLUMN

4.1 Tri-linear model and Clough model

The load-deformation relations obtained by the dynamic loading test of CFT column are in Figure 17-Figure 18. Figure 17 is the load-deformation relation in the range of small deformation before the local buckling of steel tube is generated. Figure 18 shows the load-deformation relation after the local buckling of steel tube. Before the local buckling is generated the restoring force characteristics of CFT column are spindle-shaped and approximated by the Tri-linear model as shown in Figure 17 with thin lines. The skeleton curve of this Tri-linear model shown in Figure 19 is determined by the restoring force characteristics of K_0, M_{ye}, M_{ue} obtained in the former section. After the local buckling is generated the stiffness of CFT column gradually deteriorates and the restoring force characteristics are approximated by the modified Clough model (the Clough model) [Umemura et al, 1982] as shown in Figure 18 with thin lines. The skeleton curve of this Clough model shown in Figure 20 is decided by the restoring force characteristics of K_0, M_{ue} obtained in the former section. In this figure the stiffness in the unloading state is expressed as $K_r=K_0 / \mu_m^{0.5}$ (μ_m: the maximum plastic deformation).
The restoring forces predicted by the Tri-linear model and the Clough model ($_mM_c$) are compared with the test results (M_c) as shown in Figure 21. The vertical axis in the figure means the ratio of the difference between the prediction and the test result to the ultimate strength of CFT column. In the upper figure the error ratio between the prediction and test result in the range of small deformation is shown. We can see that the prediction by the Tri-linear model is better than that by the Clough model if the deformation of column is very small. But the pre-

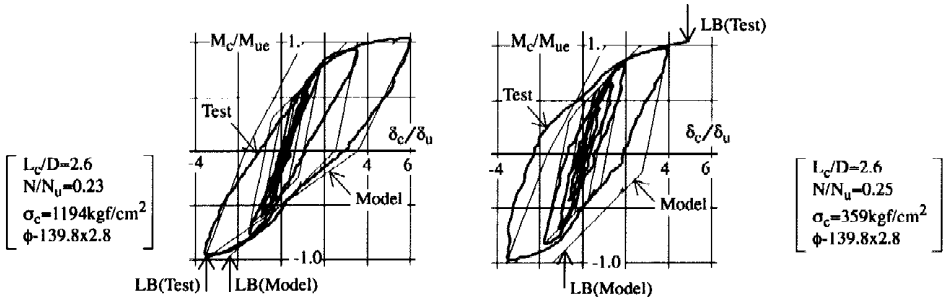

Figure 17: Load-deformation relation before local buckling of steel tube (LB: Local buckling)

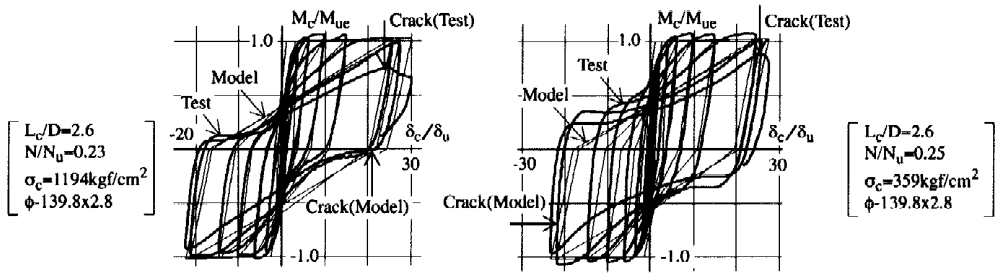

Figure 18: Load-deformation relation after local buckling of steel tube (Crack: Steel tube crack)

diction by the Clough model becomes to be better than that by the Tri-linear model as the deformation of column increases and this behavior continues until the steel tube cracks as shown in the lower figure. The boundary between the two states is not clear but at least after the local buckling of steel tube is generated, shown by LB in Figure 21, the prediction by the Clough model is better than that by the Tri-linear model.
Accordingly it is concluded that the restoring force of CFT column until the local buckling of steel tube is generated can be predicted by the Tri-linear model whose skeleton curve is defined in Figure 19 and after the local buckling of steel tube is generated the restoring force of CFT column can be well predicted by the Clough model whose skeleton curve is expressed in Figure 20. The values of stiffness in the plastic range K_1, K_2 in Figure 19-Figure 20 are assumed as $K_1=0.2K_0$, $K_2=0.001K_0$.

4.2 Error of the restoring force model

The error of the presented restoring force model is examined by calculating the energy absorbing capacity of CFT

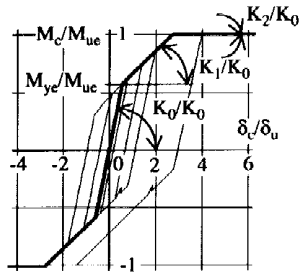

Figure 19: Skeleton curve of Tri-linear model

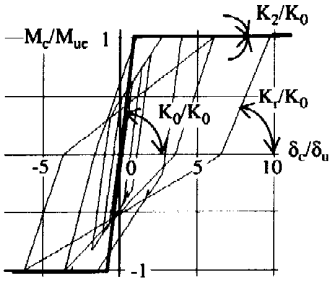

Figure 20: Skeleton curve of Clough model

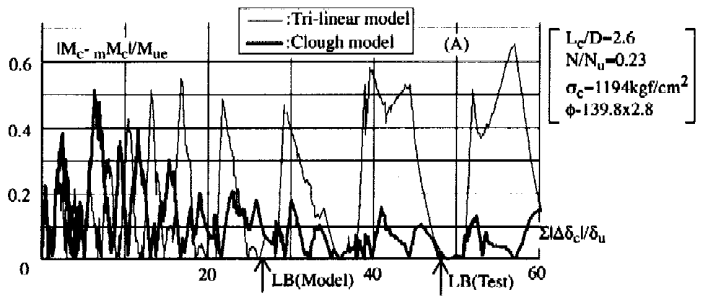

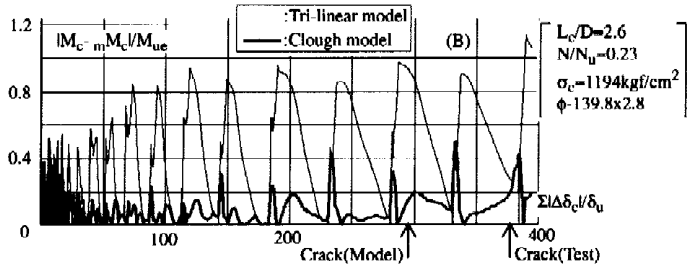

Figure 21: Approximations by the Tri-linear model and the Clough model

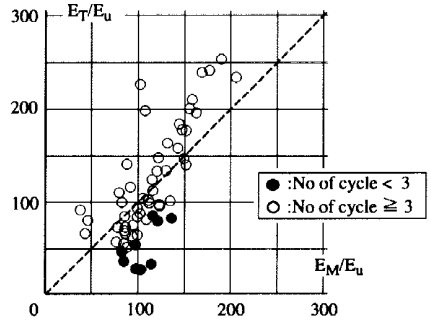

Figure 22: Energy absorbing capacity of column by the presented model and the test results

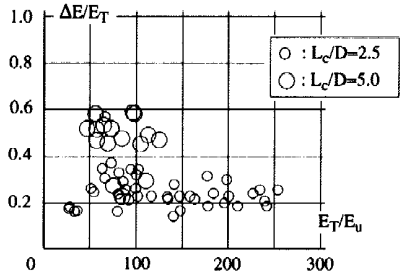

Figure 23: Average error of the presented model compared with the test results

model and comparing it with the test results. The energy absorbing capacities of CFT column E_T, E_M obtained by the test results and by the presented model are expressed by Eq.(10).

$$E_T = \Sigma M_c \Delta\delta_c / L_c$$
$$E_M = \Sigma_m M_c \Delta\delta_c / L_c \qquad (10)$$

In the calculation of E_T, Σ means the summation until the steel tube crack observed in the test and in the calculation of E_M, Σ means the summation until the ultimate state given by Eq.(9). The calculated values by Eq.(10) are shown in Figure 22 in which $E_u = M_{ue}\,\delta_u/L_c$. Figure 22 shows that the energy absorbing capacity of test is well predicted by the presented restoring force model and the value of E_M nearly corresponds to the lower limit of E_T. The errors in the calculation of the energy absorbing capacity may be compensated because the errors compared with the test results include the plus values and the minus values. From this reason the summation of the absolute difference between M_c and ${}_mM_c$ given by Eq.(11) is also examined.

$$\Delta E = \Sigma |M_c - {}_mM_c|\,|\Delta\delta_c|/L_c \qquad (11)$$

In Figure 23 the vertical axis ($\Delta E/E_T$), which is the ratio of the summation of the absolute difference by Eq.(11) to the energy absorbing capacity of test, indicates the average error of the presented model compared with the test results. According to the results in Figure 23 the average error ratio is nearly 20% in most cases.

5. CONCLUSIONS

On the basis of CFT column test it is shown that the restoring force characteristics of CFT column under cyclic load are determined by the elastic stiffness, the yield strength, the ultimate strength and the plastic deformation at the local buckling and the crack of steel tube. According to this result the restoring force model of CFT column has been obtained. The presented model is composed of the Tri-linear model and the modified Clough model whose skeleton curves are determined only by the characteristics mentioned above. Comparing with test results it is ascertained that the presented restoring force model can predict well the energy absorbing capacity of CFT column and the average error ratio of restoring force is nearly 20% in most cases.

REFERENCES

Mitsunari,K. and Saisho,M. (1996), "Ultimate Strength and Plastic Deformation Capacity of CFT Beam-Column Subjected to Dynamic Load", *11WCEE (Mexico)*, CD-ROM Paper No 414.

Saisho,M. and Mitsunari,K. (1992) "Dynamic Restoring Force Characteristics of Steel Tube Filled with Super-High Strength Concrete," *10WCEE (Madrid)*, Vol.VI, pp.3201-3204.

Saisho,M. and Mitsunari,K. (1999a), "Experimental study on ultimate behaviors of high-strength concrete filled steel tube", *Journal of Structural and Construction Engineering, AIJ*, No.520, pp133-140. (in Japanese)

Saisho,M. et al (1999b), "Ultimate bending strength of high-strength concrete filled steel tube column", *Journal of Structural and Construction Engineering, AIJ*, No.523. (in Japanese)

Saisho,M. et al(1999c), "Crack of Steel Tube and Accumulated Plastic Deformation", *Annual Meeting, AIJ*.(in Japanese)

Umemura,H. et al (1982), *Earthquake resistant design of reinforced concrete structures*, Gihoudou, Tokyo. (in Japanese)